AD-A125 666 OPTICAL COMPUTING RESEARCH(U) STANFORD UNIV CA 1/1
INFORMATION SYSTEMS LAB J W GOODMAN ET AL. 31 MAR 82
ISL-L722-7 AFOSR-TR-83-0058 AFOSR-77-3219

UNCLASSIFIED F/G 20/6 NL

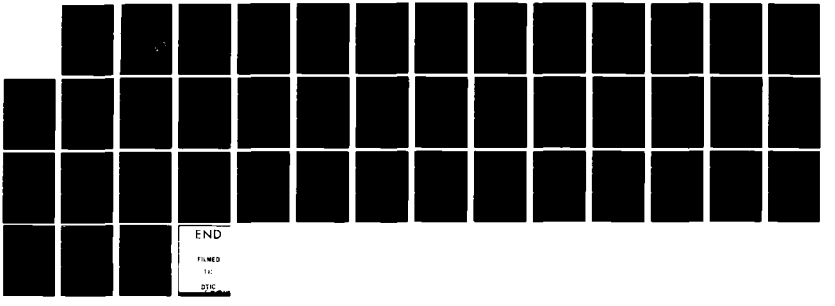

END

FILMED
1-83
DTIC

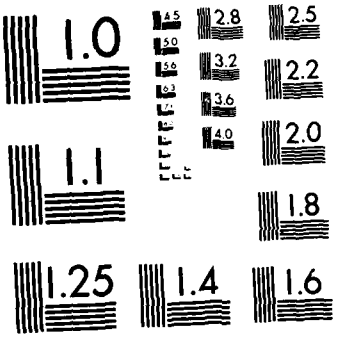

INFORMATION SYSTEMS LABORATORY

STANFORD ELECTRONICS LABORATORIES
DEPARTMENT OF ELECTRICAL ENGINEERING
STANFORD UNIVERSITY · STANFORD, CA 94305



# OPTICAL COMPUTING RESEARCH

Joseph W. Goodman
Lambertus Hesselink
Moshe Tur
Moon Song
Qizhi Cao

March 1982





Annual Technical Report No. L722-7



Research sponsored by the Air Force Office of Scientific Research, Air Force Systems Command, USAF, under Grant No. AFOSR-77-3219. The United States Government is authorized to reproduce and distribute reprints for Governmental purposes notwithstanding any copyright notation hereon.

UNCLASSIFIED

SECURITY CLASSIFICATION OF THIS PAGE (When Data Entered)

# REPORT DOCUMENTATION PAGE

READ INSTRUCTIONS BEFORE COMPLETING FORM

| | |
|---|---|
| 1. REPORT NUMBER: AFOSR-TR- 83-0058 | 2. GOVT ACCESSION NO.: AD-A125666 |
| 3. RECIPIENT'S CATALOG NUMBER: | |
| 4. TITLE (and Subtitle): Optical Computing Research | 5. TYPE OF REPORT & PERIOD COVERED: Annual Report 2-1-81 - 1-31-82 |
| | 6. PERFORMING ORG. REPORT NUMBER: |
| 7. AUTHOR(s): Joseph W. Goodman, Lambertus Hesselink, Moshe Tur, Moon Song, Qizhi Cao | 8. CONTRACT OR GRANT NUMBER(s): AFOSR-77-3219 |
| 9. PERFORMING ORGANIZATION NAME AND ADDRESS: Stanford University, Stanford, CA. 94305 | 10. PROGRAM ELEMENT, PROJECT, TASK AREA & WORK UNIT NUMBERS: 61102F 2305/B1 |
| 11. CONTROLLING OFFICE NAME AND ADDRESS: United States Air Force, Air Force Office of Scientific Research, Bldg. 410, Bolling AFB, D.C. 20332 | 12. REPORT DATE: 3-31-82 |
| | 13. NUMBER OF PAGES: 37 |
| 14. MONITORING AGENCY NAME & ADDRESS (if different from Controlling Office): As Above | 15. SECURITY CLASS. (of this report): Unclassified |
| | 15a. DECLASSIFICATION/DOWNGRADING SCHEDULE: |

16. DISTRIBUTION STATEMENT (of this Report)

Approved for public release; distribution unlimited.

17. DISTRIBUTION STATEMENT (of the abstract entered in Block 20, if different from Report)

18. SUPPLEMENTARY NOTES

19. KEY WORDS (Continue on reverse side if necessary and identify by block number)

Optical Computing
Optical Data Rocessing

20. ABSTRACT (Continue on reverse side if necessary and identify by block number)

This document contains information on the research accomplished under AFOSR Grant #AFOSR 77-3219 during the time period 1 February 1981 through 31 Jan. 1982. The work covers several different areas of optical computing research. Studies of the limitations of incoherent optical iterative processors for inversion of simultaneous linear equations are reported. Studies of methods for finding the eigenvalues and inverting circulant matrices are described. Studie of the possible use of optics for interconnections in integrated circuits, and new ideas in fiber optic signal processing are reported.

DD FORM 1 JAN 73 1473

UNCLASSIFIED

SECURITY CLASSIFICATION OF THIS PAGE (When Data Ente

# OPTICAL COMPUTING RESEARCH

Joseph W. Goodman
Lambertus Hesselink
Moshe Tur
Moon Song
Qizhi Cao



March, 1982



Annual Technical Report
No. L722-7

Research sponsored by the Air Force Office of Scientific Research, Air Force Systems Command, USAF, under Grant No. AFOSR 77-3219. The United States Government is authorized to reproduce and distribute reprints for governmental purposes not withstanding any copyright notation hereon.



Information Systems Laboratory
Stanford Electronics Laboratories
Stanford University, Stanford, California

## ABSTRACT

This document contains information on the research accomplished under AFOSR Grant No. AFOSR 77-3219 during the time period 1 February 1981 through 31 January 1982. The work covers several different areas of optical computing research. Studies of the limitations of incoherent optical iterative processors for inversion of simultaneous linear equations are reported. Studies of methods for finding the eigenvalues and inverting circulant matrices are described. Development of ideas relating to the possible use of optics for interconnections in integrated circuits are reported. Finally, new ideas in the area of fiber-optic signal processing are reported. Publications supported by the grant during the past year are also detailed.

## . INTRODUCTION

This report covers the work performed on AFOSR Grant No. 77-3219 during the time period 1 February 1981 through 31 January 1982. It is divided into 7 sections, the first of which is this Introduction. Immediately following, we summarize the results of a study of limitations of incoherent iterative optical processors, with the details presented in an appendix. Section III contains a summary on the progress on our continuing studies of coherent optical methods for finding the eigenvalues of circulant matrices and for inverting those matrices. Section IV reports the current status of our ideas related to optical interconnections for integrated circuits, including some thoughts on problems to which such techniques might be applied immediately. Section V reports the results of a short study of the multiplicative nature of speckle noise, which is part of our continuing interest in the problem of suppressing speckle noise in coherently formed images. Section VI reports ideas developed over the past year on new approaches to fiber-optic signal processing. Finally, section VII details the publications supported by the grant during the past year.

## II. LIMITATIONS OF ITERATIVE INCOHERENT OPTICAL PROCESSORS

A major effort during the past year was devoted to studies of the limitations of incoherent optical iterative processors. This work has been motivated in large measure by the earlier studies of Psaltis and Casasent[1], who proposed the use of an iterative incoherent processor for solving sets of simultaneous linear equations. The optical processor is the incoherent matrix-vector multiplier of the type developed at Stanford under this grant[2], but with the output fed back to the input.

The use of optical processors in an iterative mode raises serious questions concerning the effects of noise, non-linearities, and other defects that always plague analog systems. Our goal was to analyze the consequences of some of these defects on the performance of systems of this type. The results of this study are presented in detail in Appendix A, which is a reprint of a paper recently published in Applied Optics. The problems studied were: (1) convergence restrictions on the eigenvalues of the matrix of coefficients of the set of linear equations, and methods for relieving these restrictions; (2) effects of gain imbalance in the feedforward and feedback loops; and (3) effects of noise introduced by the successive detection processes on the convergence of the algorithm. Of these various problems, by far the least explored is the last.

In our view, the most important of the results presented is an expression that predicts the effects of noise on the performance of such a processor. Suppose that the equations to be solved are described by the matrix relation

$$\mathbf{B}\,\mathbf{x} = \mathbf{c}$$

where **B** is a matrix of coefficients, **x** is a vector of unknowns, and **c** is a known vector. Our results show that the signal-to-noise ratio at the output of the processor on the $n^{th}$ iteration is bounded by

$$(S/N)_n = (\|B^{-1}c\|)/(\|K_n\|)$$

where $B^{-1}$ is the inverse of the matrix **B**, $K_n$ is the covariance matrix of the output noise, and the $\|$ signs indicate a matrix norm. The norm of the covariance of the output noise was shown to be given by

$$\|K_n\| = \sigma^2 (1 - \|F\|^{2n+2})/(1 - \|F\|^2)$$

where **F** = I - B, I being the identity matrix. The signal to noise ratio so defined can be shown to decrease on each iteration, ultimately approaching a limiting value after many iterations.

More work needs to be done to understand the practical implications of this theoretical result. However, we anticipate that more detailed

examination will show that the limiting value of the signal-to-noise ratio will depend strongly on the spread of the eigenvalues of the matrix B, as well as on how close to the allowable convergence boundaries those eigenvalues lie. More work is planned in this area.

The reader is referred to Appendix A for the full details of the analytical treatment.

## III. OPTICAL METHODS FOR FINDING EIGENVALUES OF CIRCULANT MATRICES

For the majority of this year we have had in progress a research effort aimed at developing coherent optical techniques for finding the eigenvalues of circulant matrices. The methods are extendable to the problem of inverting such matrices as well. We describe these ideas here, and report our progress over the past 12 months.

The methods rest on the well-known fact that the discrete Fourier transform (DFT) is the linear transformation that diagonalizes any circulant matrix. The complex elements of the diagonalized matrix are the eigenvalues of the original matrix. The problem then reduces to one of modifying a coherent optical system such that the continuous Fourier transform relations ordinarily obtained between focal planes of a positive lens becomes a discrete Fourier transform. We have shown in another publication[3] that such a modification is possible if the matrix to be diagonalized is replicated several times in the front focal plane of a lens, and if the light distribution in the rear focal

plane is sampled by a discrete array of detectors. The outputs of these detectors are proportional to the squared magnitudes of the eigenvalues in question. If the full complex values are desired, interferometric detection must be performed in the rear focal plane.

Once a distribution of light amplitude proportional to the eigenvalues in question is produced, then the possibility of inverting the matrix arises. If a coherent optical light valve with an appropriate non-linear characteristic (amplitude transmittance proportional to the logarithm of incident intensity) is available, then it is possible to show that the complex amplitude of the light transmitted by such a light valve is proportional the reciprocal of the original complex eigenvalues. One further discrete Fourier transform then produces in the output plane a series of spots, each with an amplitude proportional to one element of the inverse matrix.

The conversion of a coherent optical system from one that performs continuous transforms to one that performs discrete transforms requires replication of the input matrix, as mentioned above. In addition, in order to separate the discrete spots representing the eigenvalues by amounts that make their observation easy with the naked eye, rather high resolution and minified input matrices are needed. Accordingly, a major effort was mounted to develop the capability of accurately writing replicated matrices to photographic film. In order to accomplish this goal, permission was obtained to use the DICOMED laser printer at NASA Ames Research Center. This printer can be accessed

remotely by a telephone-connected computer terminal. The end result is a transparency suitable for use in a coherent optical system.

Several circulant matrices have been created in photographic form. Each element of the matrix is encoded as an amplitude transmittance of a cell in an array of cells. Unless some form of holographic encoding is used, only non-negative and real elements can be allowed in the circulant matrix. The matrix is replicated several times, as indicated above.

Current efforts are aimed at determining the accuracy with which the desired circulant matrix has been created. To this end, the photographic recording of the matrix is scanned on a PDS digital scanner available at Stanford. The values of density and transmittance are thus read from the transparency, and compared with the values that the DICOMED printer was instructed to create. In this way we close the loop around the transparency creation process, allowing us to understand the accuracy limitations of the process. Repeatability of the exposure values has been found to range from within 4% to within 10%. By restricting the range of exposures used, we anticipate being able to operate in the region of repeatability to within 4%.

Plans for the future are centered on making measurements of the eigenvalues of a circulant matrix, and assessing the error sources and error magnitudes. Attention will also be turned in the future to studies of the matrix inversion process alluded to above.

## IV. OPTICAL INTERCONNECTIONS IN INTEGRATED CIRCUITS

Our long-standing interest in the possible use of optics for making interconnections, either from chip to chip or within a single chip, has continued during the past year. While our efforts to interest a student member of the Integrated Circuits Laboratory in working in this area have not yet been successful, nonetheless some important conceptual breakthroughs have been made in the past year. Most important amoung these has been the realization that there is a class of applications for which it is not necessary to have on the chip either optical sources or optical modulators. For these applications, we need only have detectors on the chip, a task that seems far simpler than the integration on silicon of sources or modulators (the latter task being easier with GaAs. The inclusion of detectors as part of a silicon chip seems straightforward in principle, although no doubt practical problems will be discovered when such integration is actually attempted.

Under what conditions is it useful to contemplate placing only detectors, rather than both detectors and sources/modulators, on a chip? We believe that such an approach makes sense when the chip must receive vast amounts of data from the outside world, but need only output small amounts of data. One important problem of this class has been identified during the past year. We are thinking in particular of the electronic systolic array, which is currently of considerable interest in the signal processing and VLSI communities. Consider a

simple systolic array designed to multiply a length N vector **x** by an NxN matrix B, yielding a length N output vector **y**. It is necessary to input to the processor chip the following items in the sequence described: (1) the N elements of the input vector, sequentially in time and on a single input channel; (2) the $N^2$ elements of the matrix, with as many as 2N-1 parallel channels, each carrying in time sequence the elements along one subdiagonal of the matrix. Thus the data input requirements are dominated by the necessity to have 2N parallel input channels for the matrix elements and for the input vector elements; as a consequence any such chip must have a large number of pins for inputing data, unless the chip is slowed down to allow some multiplexing on pins.

For the same chip, the data output requirements are rather modest. The N elements of the output vector appear sequentially in time and can be sent to the outside world by means of a single output pin. Thus the number of pins connecting the chip to the outside world is determined primarily by the requirements for entering data onto the chip.

Our proposed solution to this problem is illustrated in Fig. 1. The pin connections to the outside world, together with the associated bonding pads, are nearly all eliminated by the use of optical input channels. Of course pins remain for the output of data, for power to the chip, and for other necessary functions, but the brunt of the pin connection problem has been transferred to a problem of connecting to an integrated set of detectors on the chip via a series of parallel optical input channels.

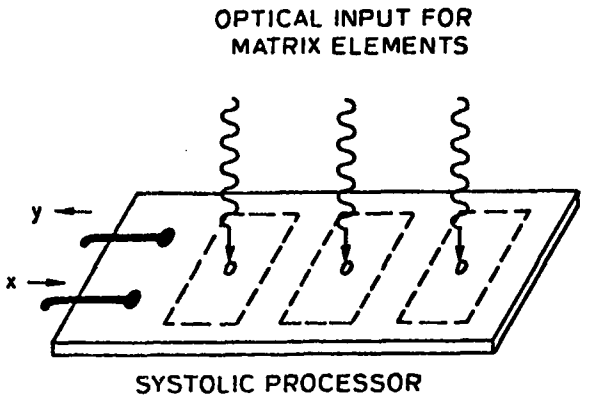


Figure 1. Input of data to a systolic array by means of optical connections.

One may well ask exactly what has been gained by converting from electronic pin connections to optical connections. The problems with the optical approach will not be fully appreciated until it has been attempted experimentaily. However, we can say the following. The problem of soldering the pin connections to bonding pads has been eliminated for those pins that are no longer necessary. This soldering process is said to be one of the most risky parts of chip manufacture. We have not eliminated the need for parallel electronic channels carrying data, for the optical sources must be driven by parallel electronic channels; rather we have transferred the requirement from on chip to off chip. The connections to the chip are non-contacting, and therefore less likely to fail. The parallel electronics for inputing

data can now be made with a larger geometrical scale than would be allowed in the on-chip environment. This fact brings both advantages and disadvantages. On the one hand the size of the opto-electronic input device may be far larger than the chip itself and more difficult to package in an extremely small space. On the other hand, the generation of the connecting optical signals on a larger geometrical scale, followed by a purely optical demagnification, may make relative alignment of the sources easier than would be the case if all work were done with the geometrical scales of the on-chip environment.

The optical approach to inputing data is certainly not without its own problems. First, and foremost, there will be an alignment problem of severe magnitude in attempting to cast the proper source images onto the proper detectors. Second, the scattering of light incident on the detectors may be of sufficient magnitude to lead to undesired cross-talk. Third, it is uncertain how small the detectors on the chip can be made. Since the optical signals involved can be of fairly high power, there is reason to hope that very small integrated detectors can be used.

Currently we are searching, together with Prof. James Meindl of the Integrated Circuits Laboratory, for a student who might undertake the task of designing and building integrated circuits that incorporate detectors for communicating with the outside world.

## V. STUDIES OF THE MULTIPLICATIVE CHARACTER OF SPECKLE

The subject of speckle and its removal from coherently formed images is one that has been of long-standing interest to us. We have spent some time during the past year investigating two subjects related to speckle. The first has consisted of a critical study of the nature of speckle noise, and an examination of the question of whether it is or is not multiplicative. A number of processing techniques have been proposed in the past that are based on the assumption that a speckled image can be regarded as the product of the ideal image intensity distribution that would be obtained if the object were not diffuse in the fine structure of its spatial transmission or reflection properties, times a speckle pattern that would be obtained if the macroscopic ideal image were spatially constant in transmission or reflection. Similar assumptions have been frequently made in modeling of speckle by numerical simulation. Our results, which are attached in preprint form as Appendix B, demonstrate that such a model is valid only if the structure of the ideal (non-diffuse) object is completely resolvable by the imaging system of concern. When this is not the case (and it is seldom true, since most objects of interest do have detail finer than the resolution capability of the optical system being used), the multiplicative model can be seriously in error. We refer the reader to Appendix B, which is scheduled for publication in APPLIED OPTICS in April, for further details.

We have also begun investigation of some new digital processing methods that we feel may have potential for suppressing speckle in coherently formed images. The suppression of speckle is a highly desirable goal, for such effects severely limit the resolution obtainable from synthetic aperture radar imagery, from acoustical imaging systems, and indeed from any coherent method of forming images. We are not yet ready to discuss our methods in detail , but we anticipate that by the time of next year's report we should have some interesting results to describe.

## VI. FIBER OPTIC SIGNAL PROCESSING

Our studies of systolic architectures in conjunction with the optical interconnection project has led to some novel concepts in the area of fiber-optic signal processing. This work was carried out in conjunction with Prof. John Shaw of the Ginzton Laboratory at Stanford. In fact the experimental evaluation of the ideas is being pursued in Prof. Shaw's group, since he has the technology to bring the ideas to fruition.

The conceptual advance that has taken place in recent months is the origination of a signal processing architecture that can be implemented using fiber optics and that is more general than a simple tapped delay line. The new processor is illustrated diagramatically in Fig. 2. We refer to it as the "double helix processor."

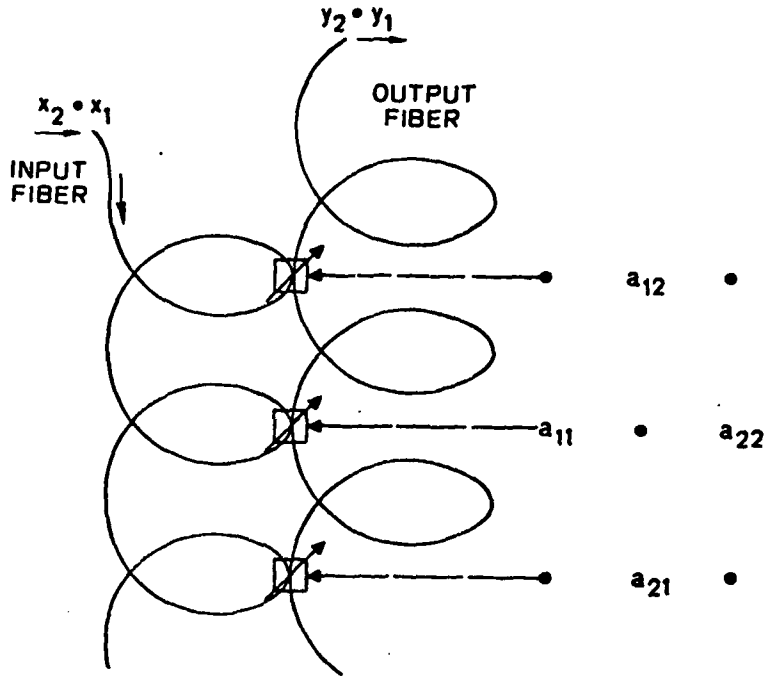


Figure 2. The double helix processor

The structure consists of two single-mode optical fibers that are connected together through a multitude of optical couplers. Input signals travel in one direction into one of the fibers, while output signals propagate in the opposite direction in the second fiber. Signals are coupled into the input fiber via intensity modulation of a laser. The output intensity modulations are detected by means of a single detector at the end of the output fiber.

This processor can be used in either a discrete or a continuous mode. In a discrete mode of operation, the input laser is modulated to emit pulses of different intensities. A sequence of N pulses represents an input vector of N elements, where it is assumed that all elements are non-negative and real. The pulses propagating out of the second fiber, if properly windowed in time, represent the N components of an output vector. The 2N-1 coupling coefficients determine the structure of the filter matrix that is realized. When the coupling

coefficients are constant in time, as would be the case with present fiber-optic technology, the matrix realized is Toeplitz, meaning that the filter is time invariant.

It is also possible to consider this processor to operate on continuous functions of time, although its impulse response is necessarily discrete. The continuously modulated input laser then enters data into the system, and the detector measures a continuous-time signal at the output.

There are a number of interesting properties of this processor. First, it can be regarded as a fiber-optic implementation of a lattice filter. The structure incorporates feedback, and as a consequence produces an impulse response that is theoretically of infinite duration. Such a filter can have both poles and zeros within the unit circle in the Z-transform domain. This result should be contrasted with the case of a simple tapped delay line, which produces an impulse response of only finite duration, and which can have only zeros within the unit circle in the Z-transform domain. Because of the "infinite impulse response" (IIR) characteristic of the double helix processor, it should allow the construction of much higher-Q filters (for a given number of couplers) than the "finite impulse response" (FIR) filter realized by a simple tapped delay line.

It is also worth mentioning that, when time-changing coupler technology becomes practical in the future, the double helix processor can be used as a systolic processor, with the input vector entered as pulses on the input fiber, and with matrix elements entered in proper

time sequence as time-changing coupling coefficients. In this case it is necessary that the coupling between the fibers be weak in order to produce the desired results.

Experimental realization of a simple double helix processor is being carried out under Prof. Shaw's funding. Results of this work will be published in a letter to OPTICS LETTERS, and credit for initiating the theoretical developments will be given to AFOSR.

## VII. PAPERS PUBLISHED AND MEETING PRESENTATIONS

We summarize in this section the various publications and presentations made during the past year under support of the grant.

### A. Papers Published

J.W. Goodman, A.R. Dias, K.M. Johnson, and D. Peri, "Parallel incoherent optical matrix-vector multipliers," Proceedings of the Workshop on Optical Signal Processing, Texas Tech University, Lubbock, Texas, 116-128 (1980). (actually published in 1981).

H.J. Caulfield, David Dvore, J.W. Goodman, and William T. Rhodes, "Eigenvector determination by noncoherent optical methods," APPLIED OPTICS 20, 2263-2265 (1981).

B. Papers Accepted for Publication

J.W. Goodman and Moon Song, "Performance limitations of an analog method for solving simultaneous linear equations," APPLIED OPTICS.

M. Tur, K.C. Chin, and J.W. Goodman, "When is Speckle Noise Multiplicative?" APPLIED OPTICS.

J.W. Goodman, "Two Generalizations of the Fourier Transform in Optical Signal Processing", **Signal transformations in optics**, S.P.I.E. Institute Series.

J.W. Goodman, "Architectural development of optical data processing systems" (invited), Australian Proc. IEE.

The above paper will also appear in the Proceedings of the Workshop on Optical Information Processing, held in Cuernevaca, Mexico, in January, 1982.

C. Oral Presentations

J.W. Goodman, "Architectural development of optical data processing systems", Workshop on Optical Information Processing, Cuernevaca, Mexico, January 1982.

Finally, the contributions of a large number of individuals to the work reported here should be acknowledged. Many contributions to the "double helix processor" concept were made by M. Tur, a Post-Doctoral Fellow partially supported by the grant. Work on the diagonalization and inversion of circulant matrices was performed by Q. Cao. The theoretical developments pertaining to the limitations of iterative processors are due almost entirely to Moon Song. Contributions to the study of speckle noise were made by M. Tur and K.C. Chin.

## REFERENCES

1. D. Psaltis, D. Casasent, and M. Carlotto, "Iterative color-multiplexed electro-optical processor," Optics Letters 4, 348 (1979).

2. Antonio R. Dias, Incoherent matrix-vector multiplication for high-speed data processing, Technical Report No. L722-4, Information Systems Laboratory, Stanford University, June 1980.

3. J.W. Goodman, "Two generalizations of the Fourier transform in optical signal processing," S.P.I.E. Institute Series (in press).

# Performance limitations of an analog method for solving simultaneous linear equations

Joseph W. Goodman and Moon S. Song

The limitations inherent in a recently proposed analog method for solving simultaneous linear equations are examined, and methods for overcoming some of these limitations are discussed. In its original form the method requires that all eigenvalues of the matrix of coefficients lie in a unit circle centered on (1,0) in the complex plane. Proper scaling of the matrix and the data vector extends this region to the entire right half of the complex plane (neglecting the effects of noise). A modification of the algorithm is described that allows the region to be further extended to the entire complex plane. If the product of the gains in the forward and feedback branches is not unity, the solution produced by the algorithm is shown to be in error. Finally, the effects of noise, which is inevitably significant in any analog realization of the algorithm, are examined. Noise is found to produce a limiting mean square error of the solution, thus preventing perfect convergence to the ideal solution vector. A procedure for determination of when to stop the iteration is proposed.

## I. Introduction

In recent publications[1,2], an iterative procedure has been described that in principle allows the solution of simultaneous linear equations by means of repeated passes through an incoherent optical system. The purpose of this paper is to point out some limitations of this particular algorithm and some methods for overcoming some of these limitations.

The method of concern is based on an incoherent optical matrix–vector multiplier described by Goodman *et al.*[3] Using such a system, Psaltis *et al.*[1] constructed an iterative processor with feedback that was designed to solve simultaneous linear equations, represented in matrix–vector form by $B\mathbf{x} = \mathbf{c}$, where $B$ is an $N \times N$ matrix of known coefficients, $\mathbf{c}$ is a length $N$ column vector of known data values, and $\mathbf{x}$ is a length $N$ column vector of unknowns. Figure 1 shows a schematic diagram of such a system. An input vector representing a trial solution enters the system via a parallel array of light-emitting diodes (LEDs). The optical system performs inner products of this input vector with the row vectors of the stored matrix mask $M$. The resulting output vector appears at the output of a parallel array of photodetectors, where it is added electronically to the known data vector $\mathbf{c}$. The result is passed back to the input of the system, where it replaces the original trial solution vector. In certain conditions this input vector converges to the solution vector desired.

As will be demonstrated, the iterative procedure in question converges only when the magnitudes of all the eigenvalues $\lambda_i$ of the matrix of coefficients lie within a unit circle centered at the point (1,0) in the complex $\lambda$ plane. In Sec. II we review these constraints in preparation for describing certain methods for relaxing them. Section III considers the question of scaling the matrix when its eigenvalues do not satisfy the necessary condition, thus in principle allowing the eigenvalues to lie anywhere in the right half of the complex $\lambda$ plane. Section IV considers a modification of the basic iteration matrix that allows extension of the procedure to equations whose matrix has eigenvalues anywhere in the complex $\lambda$ plane. Section V studies the effects of a gain mismatch in the forward and feedback paths, demonstrating that such a mismatch leads to an error in the solution. Finally, Sec. VI considers the effects of random noise, which will always be present to some degree in such systems, on the accuracy of the solution. It is shown that with noise present, the output of the system fails to converge after an infinite number of iterations, and the important problem is how to choose the number of iterations so that the solution obtained is closest to the true solution.

The authors are with Department of Electrical Engineering, Stanford University, Stanford, California 94305.

Received 8 September 1981.
0003-6935/82/030502-05$01.00/0.

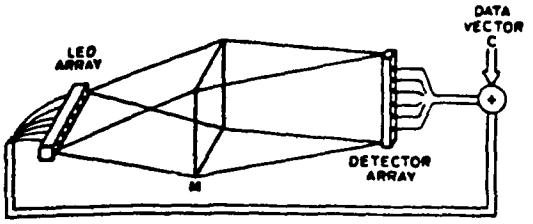


Fig. 1. Schematic diagram of an iterative optical processing system.

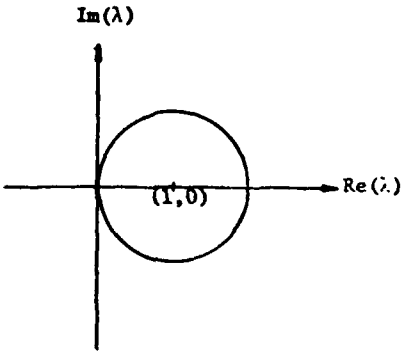


Fig. 2. Allowable region for eigenvalues in the complex plane.

## II. Convergence Conditions

Consider the problem of solving a set of linear equations described by the equation

$$B\mathbf{x} = \mathbf{c}, \tag{1}$$

where $B$ is a known $N \times N$ matrix of coefficients, $\mathbf{c}$ is a known column vector with $N$ components, and $\mathbf{x}$ is an unknown column vector of $N$ components, all of which we wish to find.

A solution for vector $\mathbf{x}$ can be found by means of an iterative algorithm[4]

$$\mathbf{x}_{n+1} = (I - B)\mathbf{x}_n + \mathbf{c}, \tag{2}$$

which can be rewritten

$$(\mathbf{x}_{n+1} - B^{-1}\mathbf{c}) = (I - B)(\mathbf{x}_n - B^{-1}\mathbf{c}), \tag{3}$$

where we have assumed that $B^{-1}$ exists.

If we let $\mathbf{y}_n = \mathbf{x}_n - B^{-1}\mathbf{c}$, we may interpret $\mathbf{y}_n$ as the deviation or error from the true solution $B^{-1}\mathbf{c}$. The error state equation can be written

$$\mathbf{y}_{n+1} = F\mathbf{y}_n, \tag{4}$$

where $F = I - B$, and the initial condition is $y_0 = \mathbf{x}_0 - B^{-1}\mathbf{c}$. The convergence condition for this iterative procedure is that $\mathbf{y}_n$ should vanish as $n$ increases:

$$\lim_{n\to\infty} \mathbf{y}_n = \lim_{n\to\infty} F^n\mathbf{y}_0 = 0 \tag{5}$$

or equivalently

$$\lim_{n\to\infty} F^n = 0. \tag{6}$$

The necessary condition for Eq. (6) to hold is that all the eigenvalues of $F$ be less than unity in magnitude,

$$|\lambda_i(F)| < 1 \text{ for } 1 \le i \le N, \tag{7}$$

or equivalently, since $\lambda_i(F) = 1 - \lambda_i(B)$,

$$|1 - \lambda_i(B)| < 1. \tag{8}$$

From Eq. (8) we see that the eigenvalues of $B$ must lie within a unit circle in the complex plane centered at the point (1,0) (see Fig. 2). In Sec. III we consider the problem of scaling the matrix to extend the class of matrices for which the algorithm will converge. In Sec. IV we consider an additional modification that allows the matrix to have eigenvalues with both positive and negative real parts.

## III. Problem of Scaling

Suppose we wish to solve a set of linear equations described by

$$B^*\mathbf{x} = \mathbf{c}^*, \tag{9}$$

where the eigenvalues of $B^*$ do not satisfy Eq. (8). Thus $|1 - \lambda_i(B^*)| \ge 1$. We introduce a real scaling factor $\alpha$ so that $|1 - \lambda_i(\alpha B^*)| < 1$. Now let $B = \alpha B^*$, $\mathbf{c} = \alpha\mathbf{c}^*$, yielding

$$(\alpha B^*)\mathbf{x} = (\alpha\mathbf{c}^*). \tag{10}$$

This new equation will have the same solution vector as the original Eq. (1). Thus by applying the iterative procedure with iteration matrix,

$$F = I - \alpha B^*, \tag{11}$$

and simultaneously scaling the data vector by the same amount, the desired solution should be obtained. By use of the scaling factor $\alpha$, the allowable region for the eigenvalues of $B$ can be extended to the entire right half of the complex $\lambda$ plane (neglecting restrictions posed by noise and speed of convergence).

While the above procedure appears straightforward, we have not yet addressed the important question as to how the scaling factor $\alpha$ should be chosen. The rate of convergence of the algorithm is dependent on the magnitude of the largest eigenvalue, which is known as the spectral radius, of the iteration matrix $F$. Therefore, to assure most rapid convergence, we should choose the scaling factor to make the magnitude of the maximum eigenvalue of the iteration matrix as small as possible. Note that small eigenvalues of $F$ are not achieved simply by choosing a small scaling factor, for as $\alpha$ approaches zero all the eigenvalues of $F$ approach unity. The convergence of the process is also limited by the presence of random measurement noise. The smaller the eigenvalues of $F$, the more significant the effects of this noise become. We defer a discussion of noise effects to Sec. VI and consider here only the optimum choice of $\alpha$ to achieve a minimum of the magnitude of the largest eigenvalue of $F$. At this point we restrict attention to the class of Hermitian matrices, so that all the eigenvalues are real. For non-Hermitian matrices, we can use the transformation method described in Sec. IV.

Noting that

$$\lambda_i(B) = \lambda_i(\alpha B^*) = \alpha\lambda_i(B^*), \tag{12}$$

we see that in passing from $B^*$ to the iteration matrix $F$, the maximum eigenvalue $\lambda_{max}(B^*)$ will be mapped

into $1 - \alpha\lambda_{max}(B^*)$, while the minimum eigenvalue $\lambda_{min}(B^*)$ will be mapped into $1 - \alpha\lambda_{min}(B^*)$. Thus to make the maximum eigenvalue of $F$ as small as possible, we should choose $\alpha$ so that the maximum and minimum eigenvalues of $F$ are equal in magnitude and opposite in sign,

$$|1 - \alpha\lambda_{min}(B^*)| = |1 - \alpha\lambda_{max}(B^*)|, \tag{13}$$

which yields an optimum value of $\alpha$ given by

$$\alpha_{opt} = \frac{2}{\lambda_{max}(B^*) + \lambda_{min}(B^*)}. \tag{14}$$

Now suppose that the spread of eigenvalues of $B^*$ is fixed at value $T \equiv \lambda_{min}(B^*)/\lambda_{max}(B^*)$. With the use of the optimum value of $\alpha$ above, we find that the magnitude of the maximum eigenvalue of the iteration matrix $F$ is given by

$$|\lambda_{max}(F)| = |1 - \alpha_{opt}\lambda_{min}(B^*)| = \left|\frac{1-r}{1+r}\right|. \tag{15}$$

This result represents the smallest achievable value of the magnitude of the eigenvalue of $F$ having largest magnitude and can be realized only by choosing the scaling constant $\alpha$ to be given by the value specified in Eq. (14).

While the above choice of $\alpha$ gives the most rapid convergence rate theoretically, we do not have the eigenvalues at hand in advance. But we can make an estimate of the maximum eigenvalue of $B$ by using the well-known Gerschgorin theorem[5] and the Schur theorem.[6] The Gerschgorin theorem states

$$\lambda_{max} \le \lambda_{bound,1} = \max_i \sum_{j=1}^{N} |b_{ij}|, \tag{16a}$$

$$\lambda_{max} \le \lambda_{bound,2} = \max_j \sum_{i=1}^{N} |b_{ij}|. \tag{16b}$$

The Schur bound gives

$$\lambda_{max} \le \lambda_{bound,3} = \left(\sum_{i=1}^{N}\sum_{j=1}^{N} b_{ij}^2\right)^{1/2}. \tag{16c}$$

Since these bounds do not impose a heavy computational load, it is reasonable to compute all of them and choose the smallest one:

$$\lambda_{max} \le \lambda_{bound} = \min|\lambda_{bound,1}, \lambda_{bound,2}, \lambda_{bound,3}|. \tag{16d}$$

But since it is not easy to estimate the upper bound of the minimum eigenvalue, it seems practically reasonable to choose the scaling factor as[7]

$$\alpha = 2/(\lambda_{bound}). \tag{17}$$

## IV. Extension to Matrices $B$ with Eigenvalues not Confined to the Right Half of the Complex Plane

We assumed in the previous discussion that all the eigenvalues of the matrix $B$ lie in the right half of the complex plane. Here we discuss further generalizations that allow matrices not satisfying this restriction to be dealt with.

First we note that if the matrix $B$ has eigenvalues that lie within a unit circle centered at $(-1,0)$ in the complex plane, a simple modification of the algorithm to

$$\mathbf{x}_{n+1} = (I + B)\mathbf{x}_n + \mathbf{c} \tag{18}$$

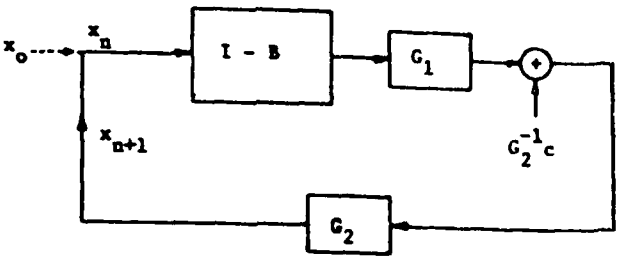


Fig. 3. Block diagram of iterative system.

allows such matrices to be dealt with. By introducing a scaling factor, the region of allowable eigenvalues can be extended to the entire left half-plane (neglecting limitations posed by noise and convergence speed).

Suppose that the matrix $B$ has some eigenvalues with positive real parts and some eigenvalues with negative real parts. Neither algorithm presented will allow such matrices to be included. However, there is a simple modification of the algorithm that will do so. Let the equation to be solved, i.e., Eq. (9), be modified by multiplying the left and right sides by the Hermitian transpose $B^{*H}$ of $B^*$, giving

$$(B^*)^H B^* \mathbf{x} = (B^*)^H \mathbf{c}^*. \tag{19}$$

The matrix $(B^*)^H B^*$ is non-negative definite (practically positive definite since $B^*$ is assumed nonsingular), and therefore the use of an iteration matrix $F = I - \alpha(B^*)^H B^*$ and a proper choice of $\alpha$ will assure that the eigenvalues of $F$ are non-negative and less than unity in magnitude. Furthermore, the solution set for Eq. (19) is precisely the same as the solution set for Eq. (9). Thus the multiplication of both the matrix $B^*$ and the data vector $\mathbf{c}^*$ by $(B^*)^H$ has generated a new equation with the same solution set but with matrix eigenvalues satisfying the necessary requirements. In this way the space of allowable eigenvalues has been extended to the entire complex plane.

## V. Effects of Gain Mismatch in the Forward and Feedback Paths

Since the optical system in question involves optical-to-electronic and electronic-to-optical conversion, and since they are analog systems, the strong possibility exists for differences of the gains in the forward and feedback paths. Figure 3 illustrates the general nature of the systems of concern. $G_1$ represents the inherent gain matrix associated with passage of the signals in the forward direction, while $G_2$ is the corresponding gain matrix in the feedback direction. The matrices are diagonal, but the elements along the diagonal need not be equal, since the different channels of an incoherent matrix–vector multiplier may have different gains.

The presence of the gain matrices $G_1$ and $G_2$ modifies Eq. (2) describing the iterative algorithm to become

$$\mathbf{x}_{n+1} = G_2 G_1 (I - B)\mathbf{x}_n + \mathbf{c}. \tag{20}$$

To see the effects of a gain mismatch, suppose that the product of gain matrices is close to the identity matrix,

$$G_2 G_1 = I + \epsilon, \tag{21}$$

where the diagonal matrix $\epsilon$ represents the gain mismatches in the various channels and is assumed to have small elements. The iteration equation becomes

$$\mathbf{x}_{n+1} = (I + \epsilon)(I - B)\mathbf{x}_n + \mathbf{c} = [I - [B - \epsilon(I - B)]]\mathbf{x}_n + \mathbf{c}. \tag{22}$$

From the above equation we can see that, when gain mismatches exist, the iterative procedure will produce a solution that is appropriate for a matrix $B - \epsilon(I - B)$ rather than the matrix $B$. We now investigate the magnitude of the errors associated with the solution vector $\mathbf{x}$.

Suppose that the iteration procedure has reached convergence; i.e.,

$$\mathbf{x}_{n+1} = \mathbf{x}_n = \mathbf{x}. \tag{23}$$

Then the iteration equation can be written

$$[I - (I + \epsilon)(I - B)]\mathbf{x} = \mathbf{c}. \tag{24}$$

Solving this equation for $\mathbf{x}$, we find

$$\mathbf{x} = [I - B^{-1}\epsilon(I - B)]^{-1}B^{-1}\mathbf{c}. \tag{25}$$

If the elements of matrix $\epsilon$ are all small, the result for $\mathbf{x}$ can be approximated as

$$\mathbf{x} \approx B^{-1}\mathbf{c} + B^{-1}\epsilon(I - B)B^{-1}\mathbf{c}. \tag{26}$$

Thus in the presence of gain mismatch, the iterative procedure converges to an incorrect answer. The error vector is given by

$$\mathbf{x}_{\text{error}} = B^{-1}\epsilon(I - B)B^{-1}\mathbf{c}. \tag{27}$$

The relative size of the error due to gain mismatch can be written (assuming a symmetric $B$)

$$\begin{aligned}\frac{\|\mathbf{x}_{\text{error}}\|}{\|B^{-1}\mathbf{c}\|} &= \frac{\|B^{-1}\epsilon(I - B)B^{-1}\mathbf{c}\|}{\|B^{-1}\mathbf{c}\|} \\ &\le \frac{\|B^{-1}\epsilon(I - B)\| \cdot \|B^{-1}\mathbf{c}\|}{\|B^{-1}\mathbf{c}\|} \\ &\le \|\epsilon\| \cdot \|B^{-1} - I\| \le \|\epsilon\| \cdot (\|B^{-1}\| + 1),\end{aligned} \tag{28}$$

where $\|\cdot\|$ indicates a matrix norm, defined by

$$\|K\| \equiv |\text{largest eigenvalue of } K^H K|^{1/2}, \tag{29}$$

and the superscript $H$ indicates a Hermitian transpose. Thus as might be expected, the bound on the relative error is proportional to the gain mismatch $\|\epsilon\|$ and to $\|B^{-1}\|$ (which is essentially the inverse of the smallest eigenvalue of $B$).

## VI. Effects of Noise on the Convergence of the Algorithm

When an iterative procedure such as that of interest here is implemented with an analog system, concern naturally arises as to the effects of noise. Noise is introduced on every pass through the loop, and it should be expected that its effects will eventually build up to the point where they cannot be neglected. Our purpose here is to examine the effects of noise in as quantitative a way as possible.

We make the approximation that the noise involved is purely additive, and we further assume that it has zero mean. Figure 4 shows a block diagram of the system considered. The state equation with a noise component present must be rewritten as

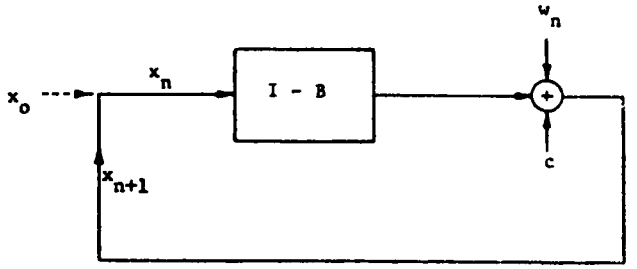


Fig. 4. Block diagram of system with noise.

$$\mathbf{x}_{n+1} = (I - B)\mathbf{x}_n + \mathbf{c} + \mathbf{w}_n, \tag{30}$$

where $\mathbf{w}_n$ is the noise vector of concern. The error state equation becomes

$$\mathbf{y}_{n+1} = F\mathbf{y}_n + \mathbf{w}_n, \tag{31}$$

where again we have used the definition $\mathbf{y}_n = \mathbf{x}_n - B^{-1}\mathbf{c}$.

The solution of Eq. (30) can be divided into two components: (1) a deterministic homogeneous solution $\hat{\mathbf{y}}_n$ due to the initial condition, and (2) a stochastic particular solution $\tilde{\mathbf{y}}_n$ due to the noise input. Since the system is linear, we may consider these components separately. Note that $\hat{\mathbf{y}}_n$ is the solution to

$$\hat{\mathbf{y}}_{n+1} = F\hat{\mathbf{y}}_n \tag{32}$$

with $\hat{\mathbf{y}}_0 = \mathbf{x}_0 - \mathrm{B}^{-1}\mathbf{c}$, while $\tilde{\mathbf{y}}_n$ is the solution to

$$\tilde{\mathbf{y}}_{n+1} = F\tilde{\mathbf{y}}_n + \mathbf{w}_n \tag{33}$$

with $\tilde{\mathbf{y}}_0 = 0$. The complete solution is given by

$$\mathbf{y}_n = \hat{\mathbf{y}}_n + \tilde{\mathbf{y}}_n. \tag{34}$$

The homogeneous part of the solution was analyzed in the earlier sections. Here we consider only the noisy part $\tilde{\mathbf{y}}_n$.

From Eq. (33) we write

$$\tilde{\mathbf{y}}_{n+1} = F\tilde{\mathbf{y}}_n + \mathbf{w}_n = \sum_{k=0}^{n} F^{n-k}\mathbf{w}_k. \tag{35}$$

Squaring both sides of this equation and taking averages with the assumption that the noise is both white and stationary yield the following expression for the covariance matrix of the noise output.

$$K_{n+1} \equiv E(\tilde{\mathbf{y}}_{n+1}\tilde{\mathbf{y}}_{n+1}^H) = \sigma^2 \sum_{k=0}^{n} (FF^H)^k, \tag{36}$$

where $\sigma^2 I$ is the covariance of noise vector $\mathbf{w}_n$.

Using the definition of matrix norm in Eq. (29), the following inequality can be used to put a bound on the error covariance:

$$\|K_n\| \le \sigma^2 \sum_{k=0}^{n} \|F\|^{2k} = \sigma^2 \frac{1 - \|F\|^{2n+2}}{1 - \|F\|^2}. \tag{37}$$

With the above result in mind, we define a time varying $(\text{SNR})_n$ by

$$(\text{SNR})_n = \frac{\|B^{-1}\mathbf{c}\|}{\sqrt{\|K_n\|}}. \tag{38}$$

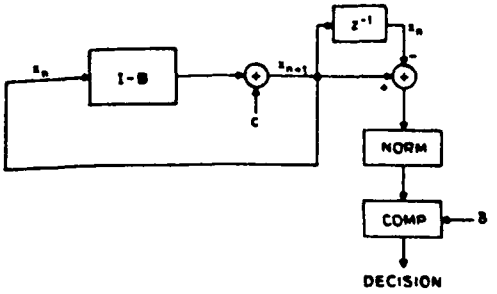


Fig. 5. Block diagram of system with criterion to stop.

From Eq. (38) we see that, due to the increasing nature of $\|K_n\|$ with iteration number, the $(SNR)_n$ becomes smaller at each iteration. Furthermore, when the norm $\|F\|$ is less than one, the $(SNR)_n$ ultimately approaches a limiting value that is independent of the iteration number.

During the initial iterations, the starting condition will be sufficiently far from the true solution that the deterministic component of error will dominate, and the output vector will start to move toward the solution vector. The error will therefore begin to decrease. As the iteration number grows, the noise component of the output builds up, and eventually it becomes the dominant component of error, preventing the error from vanishing. Thus the process initially converges, but then the mean square error approaches a nonzero asymptotic value. A key question concerns the means for judging when to stop the iteration. When the process is sufficiently slow to allow a human observer to interact with the system, judgment can perhaps be made as to when to terminate the procedure. However, interest is greater when the processing speed is high, and in such cases the possibility of human intervention vanishes. An automatic means for judging when to terminate the iteration is needed. We now describe one such method.

Suppose we obtain on a particular iteration a solution $\bar{\mathbf{x}}$ which may differ from the true solution $B^{-1}\mathbf{c}$. Obviously, it is our hope that $\bar{\mathbf{x}}$ will satisfy the given equation as closely as possible, i.e., that

$$B\bar{\mathbf{x}} = \mathbf{c}. \tag{39}$$

Thus our efforts to solve the equation are equivalent to the minimization of the equation error, $\mathbf{c} - B\bar{\mathbf{x}}$, which will be zero if $\bar{\mathbf{x}}$ happens to be $B^{-1}\mathbf{c}$. Hence we can use this error as a measure of closeness to the solution. Let the equation error associated with solution $\mathbf{x}_n$ be represented by $\mathbf{e}_n$; i.e.,

$$\mathbf{e}_n = \mathbf{c} - B\mathbf{x}_n. \tag{40}$$

Then it is easy to demonstrate that $\mathbf{e}_n$ satisfies

$$\mathbf{e}_{n+1} = F\mathbf{e}_n \tag{41}$$

with the initial condition $\mathbf{e}_0 = \mathbf{c} - B\mathbf{x}_0$. If $B$ and $\mathbf{c}$ have been properly scaled so that $F$ is a stable matrix, we see that $\mathbf{e}_n$ should vanish as the iteration proceeds

$$\lim_{n\to\infty} \mathbf{e}_n = \lim_{n\to\infty} F^n\mathbf{e}_0 = 0. \tag{42}$$

We can monitor the equation error at each iteration by measuring some form of the vector norm of $\mathbf{e}_n$. (One easy method would be by taking the absolute value of the maximum component of $\mathbf{e}_n$.) This quantity thus provides the required estimate of closeness to the true solution.

The last question is: how can we obtain the equation error experimentally? If we note that

$$\mathbf{x}_{n+1} = \mathbf{x}_n - B\mathbf{x}_n + \mathbf{c} = \mathbf{x}_n + \mathbf{e}_n, \tag{43}$$

which is readily available after the $(n+1)$st iteration, we can obtain $\mathbf{e}_n$ simply by subtracting $\mathbf{x}_n$ from $\mathbf{x}_{n+1}$. The system then must contain a means for storing one vector $\mathbf{x}_n$. A block diagram of the method is illustrated in Fig. 5.

## VII. Conclusions

We have discussed some performance limitations of a certain optical implementation of an iterative algorithm that can be used to solve simultaneous linear equations. The method, as originally proposed, requires that all eigenvalues of the matrix of coefficients lie within a circle in the complex plane having a unit radius and centered on the point (1,0). We have described a method for modifing the matrix and the data vector so that the eigenvalues of the matrix of interest can (in principle) lie anywhere in the complex plane. It has been shown that a difference in gains associated with the forward and feedback paths causes the algorithm to converge to an incorrect solution vector. The effects of measurement noise on the algorithm have also been examined. It has been shown that the presence of noise affects the convergence of the algorithm, leading to a mean square error between the true solution vector and the experimental solution vector that fails to vanish as the iteration number grows large. Finally, we have suggested a means for determining when the iterations should be stopped, based on the difference between the solution vectors on two successive iterations. All the above considerations are of considerable importance when the algorithm is implemented by means of an analog optical system.

The work described here was supported by the Air Force Office of Scientific Research.

## References

1. D. Psaltis, D. Casasent, and M. Carlotto, Opt. Lett., 4, 348 (1979).
2. H. Maitre, Comput. Graphics Image Process. 16, No. 2, 95 (1981).
3. J. W. Goodman, A. R. Dias, and L. M. Woody, Opt. Lett. 2, 1 (1978).
4. G. Strang, *Linear Algebra and its Applications* (Academic, New York, 1976), p. 297.
5. R. J. Goult *et al.*, *Computational Method in Linear Algebra* (Wiley, New York, 1974), pp. 93, 159–160.
6. E. Kreyszig, *Advanced Engineering Mathematics* (Wiley, New York, 1979), p. 823.
7. There is a subtlety that should be mentioned. If $\lambda_{bound}$ happens to equal exactly $\lambda_{max}$, choice (17) for $\alpha$ yields a maximum eigenvalue of unity for the iteration matrix. To be safe, $\alpha$ should be chosen somewhat smaller than Eq. (17).

APPENDIX B

# WHEN IS SPECKLE NOISE MULTIPLICATIVE?

*M. Tur*

*K. C. Chin**

*J. W. Goodman*

Information System Laboratory, Stanford University, Stanford, Ca. 94305

In coherent illumination, objects with roughness on the order of a wavelength cause speckle to appear in their images as formed by imaging systems which cannot resolve the microscale of the objects' roughness [1]. Thus, when a laser illuminates a composite object composed of a diffuser (whose complex amplitude transmittance is $d(x',y')$) in contact with a transparency $t(x',y')$ (see Fig. 1) the spatial intensity distribution in the image plane will be very noisy (i.e. speckled ), provided the amplitude point spread function of the optical system is broad by comparison with the microscopic surface variations of the diffuser. Recent publications [2]-[4] as well as older ones [5]-[7] have assumed that speckle noise is multiplicative, i. e.

$$I_{ts}(x,y) = \alpha \cdot I_{inc}(x,y) \cdot I_s(x,y) \tag{1}$$

where: $I_{ts}(x,y)$ is the (random) spatial intensity distribution in the speckled image of the transparency $t(x',y')$, $I_s(x,y)$ is the intensity distribution in the image of the diffuser alone ( $t(x',y') = 1$ ) and $I_{inc}(x,y)$ is the incoherent image of the transparency $t(x',y')$. The proportionality factor $\alpha$ depends on the system parameters. Eq. (1) is mainly based on the work of Lowenthal and Arsenault [8], who showed that when $d(x',y')$ is a stationary, $\delta$ correlated random process with independent real and imaginary parts having zero means and the same

*On leave from the Dept. of Physics, Beijing University, People's Republic of China.

variances, the *mean* and *standard deviation* of $I_{ts}(x,y)$ are equal to $I_{inc}(x,y)$. That is,

$$\langle I_{ts}(x,y)\rangle = I_{inc}(x,y) \;:\; \langle I_{ts}^2(x,y)\rangle = 2I_{inc}^2(x,y) \tag{2}$$

where $\langle\ \rangle$ denote an ensemble average over different realizations of the diffuser and/or the illumination. Using Eqs. (1)-(2), we also find that $\alpha$ in Eq. (1) is given by: $\alpha = \langle I_s(x,y)\rangle^{-1}$. While Lim and Nawab [2] specifically restricted their multiplicative model to the case when the degraded image has been sampled coarsely enough such that the degradation at any point can be assumed to be independent of that at all other points, most other investigators have used Eq. (1) without further limitations.

It is the purpose of this letter to point out that Eq. (1) is only an approximation which is certainly not valid when the transparency $t(x',y')$ has spatial details which cannot be resolved by the coherent system. This observation is of practical importance since most objects contain fine details well beyond the resolution capabilities of the systems that are used to image them.

Due to the finite resolving power of the imaging system, the complex wave amplitude $\mathbf{U}$ at the image point $P$ (see Fig. 1) is the result of a coherent addition of contributions from many independent areas within a finite patch $R_{cell}$ which is of the order of a resolution cell. The (random) intensity at $P=(x_p,y_p)$ is given by

$$I_{ts}(x_p,y_p) = |\mathbf{U}(x_p,y_p)|^2 = \left| \iint_{R_{cell}} dx'\,dy'\,h(x_p-x',y_p-y')\,t(x',y')\exp[i\varphi(x',y')] \right|^2 \tag{3}$$

where $h(x,y)$ is the amplitude impulse response of the system (assuming unity magnification) and $\varphi(x',y')$ is a random phase delay which is introduced by the diffuser at the object point $(x',y')$ : $d(x',y') = \exp[i\varphi(x'y')]$. Obviously, when $t(x',y')$ does not change appreciably within $R_{cell}$, Eq. (3) reduces to

$$I_{ts}(x_p,y_p) = |t(x_p,y_p)|^2 \cdot \left| \iint_{R_{cell}} dx'\, dy'\, h(x_p-x',y_p-y') \exp[i\varphi(x',y')] \right|^2 \qquad (4)$$

Since in this limiting case $I_{inc}(x_p,y_p) \alpha |t(x_p,y_p)|^2$ and the second factor on the right hand side of Eq. (≒) is $I_s(x_p,y_p)$, Eq. (4) has the same form as Eq. (1). This explains why Lee [3] was successful in verifying Eq. (1) for the *flat* areas in his synthetic aperture radar images. However, when $t(x',y')$ has spatial details smaller than or comparable to $R_{cell}$, Eq. (1) is no longer valid. As an example, consider the case of a sharp opaque edge object and denote by $I_{ts}$ the speckled (random) intensity at the geometrical image of the edge $G$ (see Fig. 2) and by $I_s$ the intensity of the speckle at the same point in the absence of the sharp edge. Based on a random walk model [9], $I_s$ is the intensity of the sum of two independent random walks $Z^+$ and $Z^-$ originated respectively from $R^+_{cell}$ and $R^-_{cell}$ in Fig. 2. Obviously, $I_{ts}$ is the intensity of $Z^+$. Assuming exponential distributions for the intensities, it is readily shown that the joint probability density function for $I_{ts}$ and $I_s$ is given by:

$$p(I_s,I_{ts}) = \frac{1}{[\,<I_s>-<I_{ts}>\,]<I_{ts}>} \exp\left[-\frac{<I_{ts}>I_s+<I_s>I_{ts}}{[\,<I_s>-<I_{ts}>\,]<I_{ts}>}\right] I_0\left[2\frac{\sqrt{I_s I_{ts}}}{[\,<I_s>-<I_{ts}>\,]}\right] \qquad (5)$$

where $<I_s>$ and $<I_{ts}>$ are the ensemble averages of $I_s$ and $I_{ts}$, and $I_0$ is a modified Bessel function of the first kind, zero order. Therefore, the quotient $Q = \sqrt{\frac{I_s}{I_{ts}}}$ *,assumed constant in* Eq. (1), is instead a continuously distributed quantity with a probability density given by:

$$p(Q) = 2Q\frac{(B-1)Q^2 + B(B-1)}{\left[Q^4+2(B-2)Q^2+B^2\right]^{\frac{3}{2}}} \qquad (6)$$

where $B = \frac{<I_s>}{<I_{ts}>}$ (In the simplest case, when $R_{cell}$ is equally divided by the edge, $B=2$). Since for large values of $Q$, $p(Q) \approx Q^{-3}$, $Q$ has an infinite

variance which means that the zeroes of $I_{ts}$ occur *independently* of those of $I_s$, in contradiction to Eq. (1).

To further validate our assertion, we have carried out one-dimensional numerical simulations of the image forming system of Fig. 1 for slanted objects with different slopes. The speckled image was generated using convolution techniques rather than Fourier domain methods. Results for $\frac{I_s}{I_{ts}}$ near the point $G$ in Fig. 2, show that for two different realizations of the diffuser, the steeper the edge, the larger the difference between the two realizations. We have also confirmed that for $B = 2$, $<\left[\frac{I_s}{I_{ts}}\right]^{\frac{1}{2}}>$ assumes the value 1.91 which is the first moment of the distribution $p(Q)$, Eq. (6).

A statistical estimate for the error introduced by the multiplicative model can be obtained from the mean square error $M(x,y)$:

$$M(x,y) = <\left[I_{ts}(x,y) - \alpha \cdot I_{inc}(x,y) \cdot I_s(x,y)\right]^2> \tag{7}$$

In order to evaluate $M$ we follow the assumptions and results of Lowenthal and Arsenault [8], so that Eq. (7) reduces to:

$$M(x,y) = 2I_{inc}^2(x,y)\left[2 - \frac{<I_{ts}(x,y) \cdot I_s(x,y)>}{I_{inc}(x,y) \cdot <I_s(x,y)>}\right] \tag{8}$$

Using the above assumptions together with the additional fact that the complex wave amplitudes $\mathbf{U}_{ts}$ and $\mathbf{U}_s$ at the image point $(x,y)$, originate from the same diffuser, we may conclude that $\mathbf{U}_{ts}(x,y)$ and $\mathbf{U}_s(x,y)$ are two complex mutually circular Gaussian random variables, and therefore:

$$\begin{aligned} <I_{ts}(x,y) \cdot I_s(x,y)> &= <\mathbf{U}_{ts}(x,y)\mathbf{U}_{ts}^*(x,y)\mathbf{U}_s(x,y)\mathbf{U}_s^*(x,y)> \\ &= I_{inc}(x,y) \cdot <I_s(x,y)> + \left|<\mathbf{U}_{ts}(x,y)\mathbf{U}_s^*(x,y)>\right|^2 \end{aligned} \tag{9}$$

The star denotes complex conjugation. Substituting Eq. (9) in Eq. (8), we find:

$$M(x,y) = 2I_{inc}^2(x,y)\left[1 - \frac{\left|\langle U_{ts}(x,y)U_s^*(x,y)\rangle\right|^2}{I_{inc}(x,y)\cdot\langle I_s(x,y)\rangle}\right] \tag{10}$$

Recalling that $\langle d(x_1',y_1')d(x_2',y_2')\rangle = \delta(x_1'-x_2')\delta(y_1'-y_2')$ and that $|d(x',y')| = 1$, Eq. (10) may be rewritten as:

$$\frac{M(x,y)}{2I_{inc}^2(x,y)} = 1 - \frac{\left|\int_{-\infty}^{+\infty}\int dx'\,dy'\,t(x',y')\,|h(x-x',y-y')|^2\right|^2}{\int_{-\infty}^{+\infty}\int dx'\,dy'\,|t(x',y')|^2\cdot|h(x-x',y-y')|^2\cdot\int_{-\infty}^{+\infty}\int dx'\,dy'\,|h(x-x',y-y')|^2} \tag{11}$$

Due to Schwart's inequality, $0 \le M(x,y) \le 1$. Moreover, using the condition for equality in Schwartz's inequality, the multiplicative model holds, i.e. $M=0$, if and only if $t(x',y')$ is constant over the resolution cell of the system (where $h(x-x',y-y') \neq 0$).

Figures 3 and 4 describe the spatial distributions of $M(x,y)$ and $I_{inc}(x,y)$ for a sharp edge as well as for slanted (see insert in Fig.4) objects, as obtained from an imaging system with unit magnification and a square aperture. It is readily seen that far from the edge $M$ approaches zero. Also, as the slope of the object decreases, so does $M$.

We have thus shown that the multiplicative model fails when the object contains fine details which cannot be resolved by the imaging system.

## ACKNOWLEDGEMENTS

This work was supported in part by the Air Force Office of Scientific Research. M. Tur would like to acknowledge the support of a Rotschild and a Fullbright Fellowships.

## REFERENCES


1. J. C. Dainty, Ed., *Laser Speckle and Related Phenomena*, Vol. 9 of *Topics in Applied Physics*, Springer Verlag (1975)
2. J. S. Lim and H. Nawab, Opt. Eng.,**20**, 472-480(1981)
3. J. S. Lee, Computer Graphics and Image Processing,**17**, 24-32(1981)
4. A. K. Jain and C. R. Christensen, Proc. SPIE Conf. on *Applications of Speckle Phenomena*, Vol. 243, 46-50(1980)
5. H. Kato and J. W. Goodman, Appl. Opt.,**14**, 1813-1823(1975)
6. H. H. Arsenault and G. April, J. Opt. Soc. Am., **66**, 1160-1163(1976)
7. C. R. Christensen *et. al*, "Object detectability in speckle noise", International Conf. on Lasers, Orlando, Florida, Dec. 1978.
8. S. Lowenthal and H. Arsenault, J. Opt. Soc. Am., **60**,1478-1483(1970)
9. J. W. Goodman, in Ref. [1].

## Figure Captions

Figure 1: The optical system. $d(x',y')$ and $t(x',y')$ are, respectively, the complex transmittances of the diffuser and the object transparency.

Figure 2: Same as Fig. 1 but with a sharp edge object. $R_{cell}^{-}$ is the part of the system's resolution cell ( $R_{cell}$ ) which is blocked by the object.

Figure 3: The spatial variation of $M(x,y)$ for a sharp edge object. The incoherent image of the sharp edge is also included. The abscissa is scaled by the transverse dimension of $R_{cell}$ . $\lambda$ is the wavelength, $f$ is the focal length of the imaging system and $\alpha$ is the size of its square aperture.

Figure 4: Same as Fig. 3, but for two slanted objects (see insert). While the change in object 1 occurs on a scale comparable to $R_{cell}$ , object 2 is fully resolved by the system. The incoherent impulse response of the system is also included in the insert.

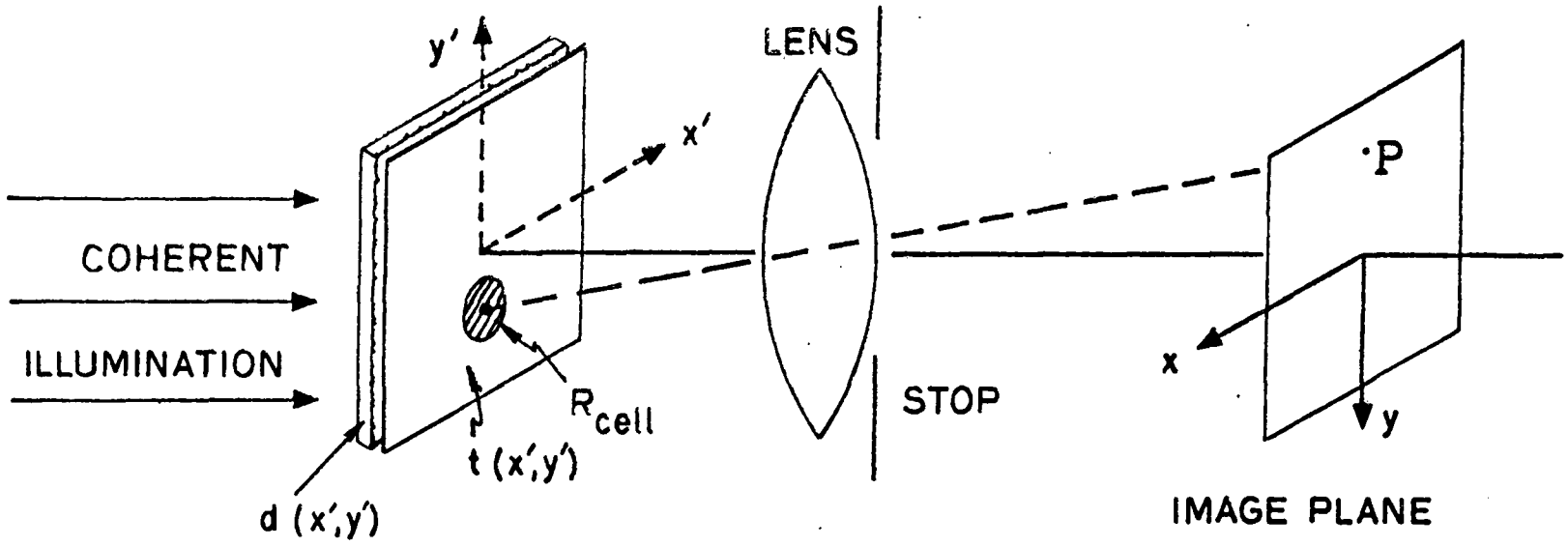
y'
x'
LENS
·P
COHERENT
ILLUMINATION
$R_{cell}$
STOP
x
y
t (x',y')
d (x',y')
IMAGE PLANE

FIGURE 1

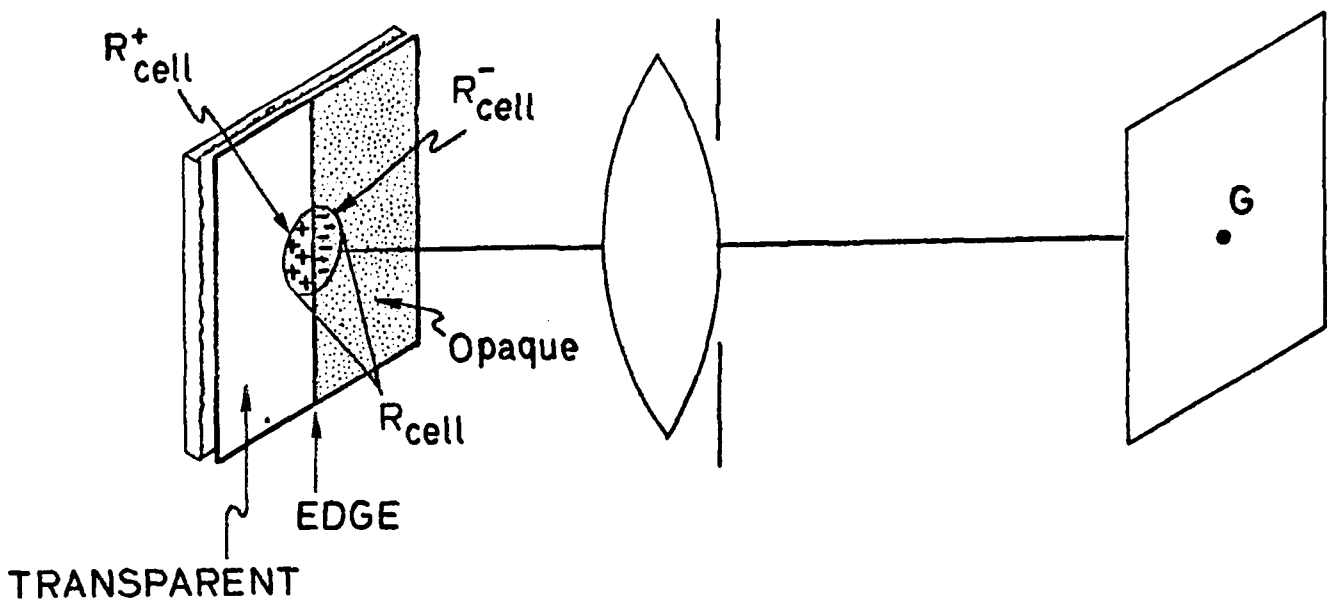


FIGURE 2

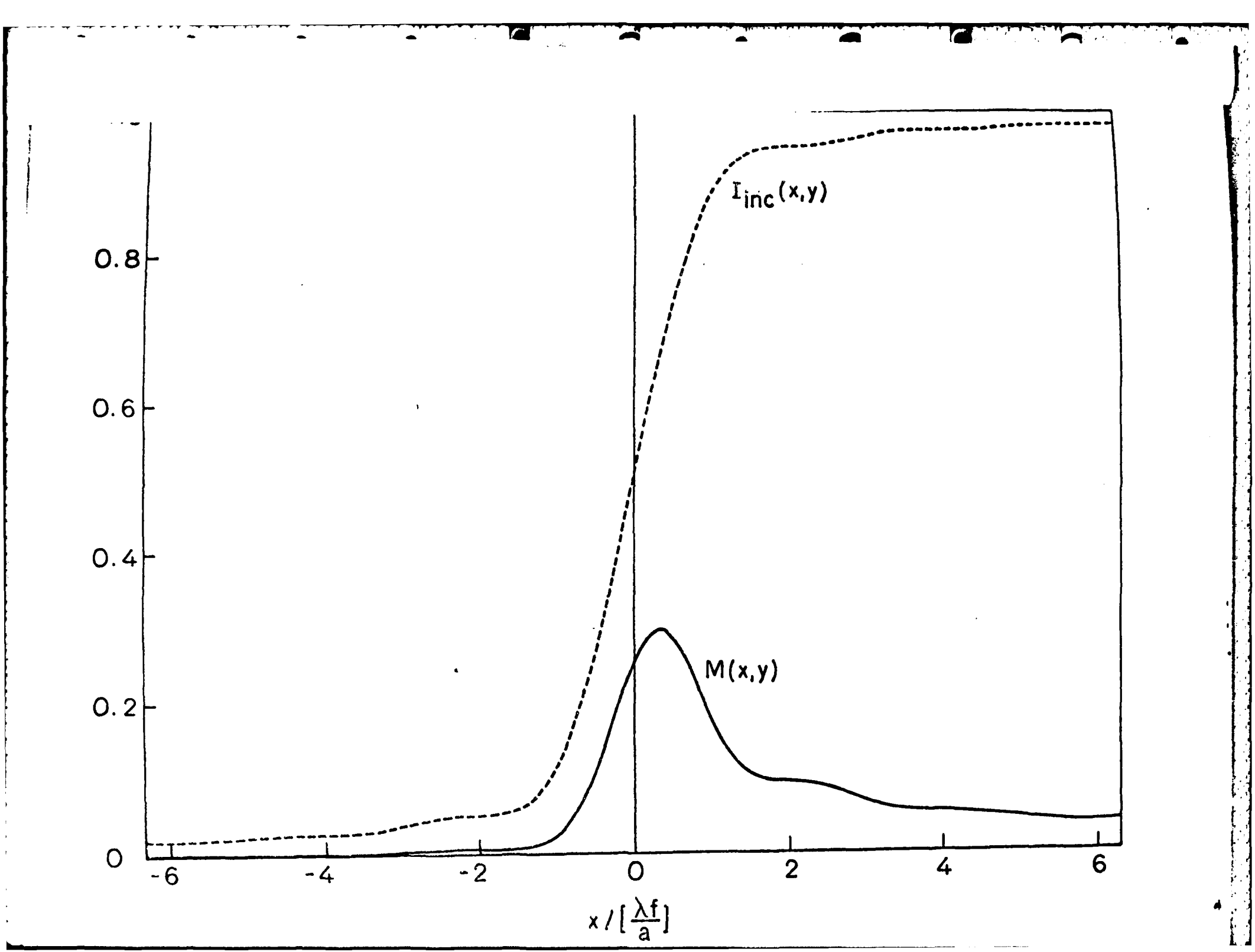
$I_{inc}(x,y)$
M(x,y)
0.8
0.6
0.4
0.2
0
-6
-4
-2
0
2
4
6
$x/[\frac{\lambda f}{a}]$

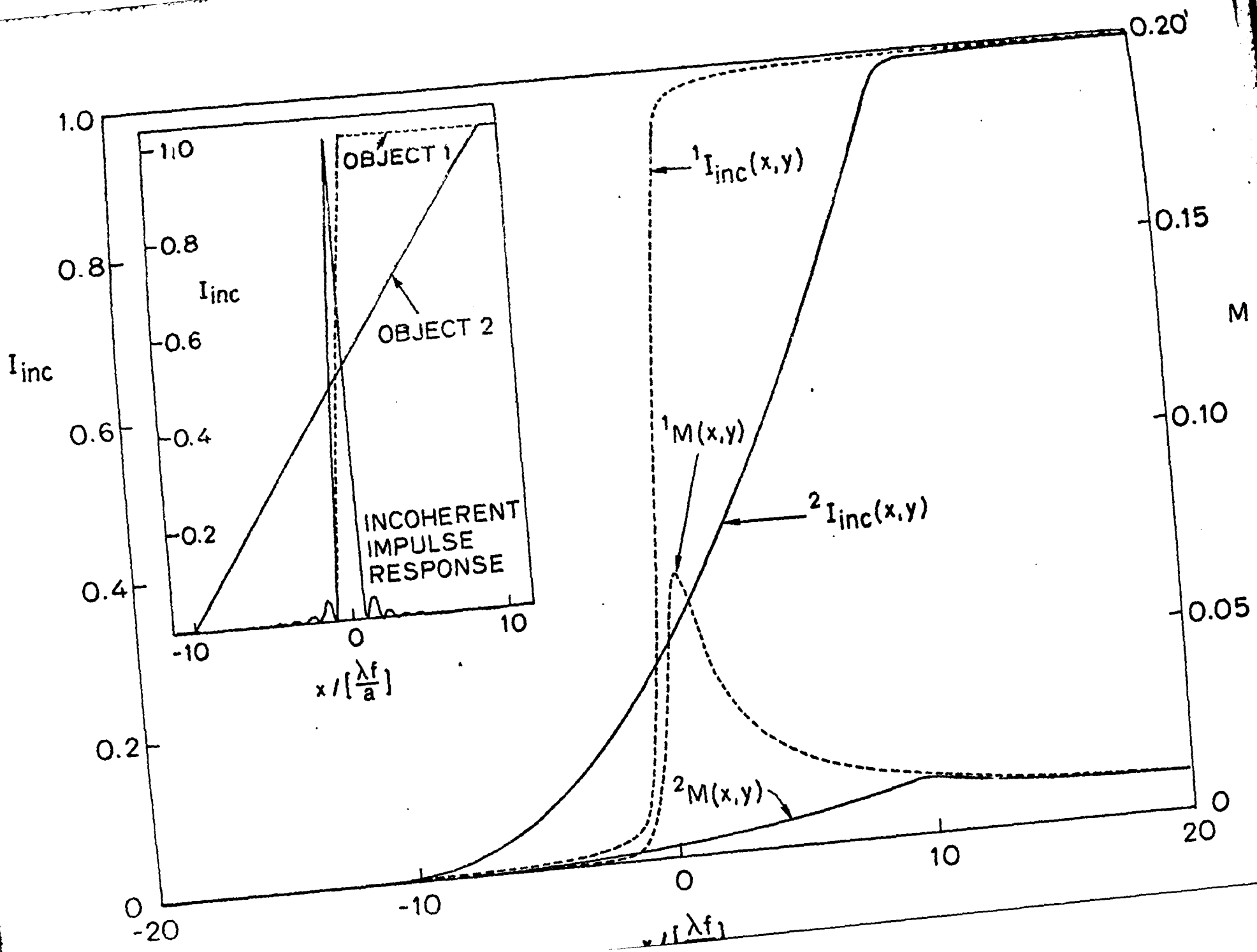
1.0
0.8
0.6
0.4
0.2
0
$I_{inc}$
-20
-10
0
10
20
$x/[\frac{\lambda f}{a}]$
$^1I_{inc}(x,y)$
$^2I_{inc}(x,y)$
$^1M(x,y)$
$^2M(x,y)$
0.20
0.15
0.10
0.05
0
M
1.0
0.8
0.6
0.4
0.2
$I_{inc}$
OBJECT 1
OBJECT 2
INCOHERENT
IMPULSE
RESPONSE
-10
0
10
$x/[\frac{\lambda f}{a}]$

## AFOSR Contractors and Grantees

Dr David Casasent
Carnegie-Mellon University
Department of Electrical Engineering
Pittsburgh, Pennsylvania 15213

Dr George Eichmann
Department of Electrical Engineering
The City University of New York
Covent Avenue at 138th Street
New York, N.Y. 10031

Dr Elsa Garmire
Center for Laser Studies
University of Southern California
Los Angeles, California 90007

Dr Nicholas George
Director, Institute of Optics
The University of Rochester
Rochester, New York 14627

Dr Joseph W. Goodman
Department of Electrical Engineering
Stanford Electronics Laboratories
Stanford University
Stanford, California 94305

Dr Bobby R. Hunt
Systems & Industrial Engineering Dept
University of Arizona
Tucson, Arizona 85721

Dr.Peter Kellman
ESL Incorporated
495 Java Drive
Sunnyvale, California 94086

Dr Sing H. Lee
Dept of Applied Physics and Information Science
University of California, San Diego
La Jolla, California 92093

Mr Kenneth Leib
Research Department
Grumman Aerospace Corporation
South Oyster Bay Road
Bethpage, New York 11714

Prof Emmett N. Leith
Electrical and Computer Engineering Dept
The University of Michigan
Ann Arbor, Michigan 48109

Dr William T. Rhodes
School of Electrical Engineering
Georgia Institute of Technology
Atlanta, Georgia 30332

Dr Alexander A. Sawchuk
Electrical Engineering Dept
University of Southern California
Los Angeles, California 90007

Mr Bernard Soffer
Opto-Electronics Department
Hughes Research Laboratories
3011 Malibu Canyon Road
Malibu, California 90265

Dr William Steier
Co-Chairman, Electrical Engineering Dept
University of Southern California
Los Angeles, California 90007

Dr C. S. Tsai
Department of Electrical Engineering
Carnegie-Mellon University
Pittsburgh, Pennsylvania 15213

Dr John Walkup
Department of Electrical Engineering
Texas Tech University
Lubbock, Texas 79409

Dr Cardinal Warde
Electrical Engineering & Computer Science
Massachusetts Institute of Technology
Cambridge, Massachusetts 02139

Supplemental Distribution List

Dr Gerald Brandt
Westinghouse Research & Development Center
1310 Beulah Road
Pittsburgh, Pennsylvania 15235

Dr Keith Bromley
Naval Ocean Systems Center
Code 8111
271 Catalina Blvd
San Diego, California 92152

Dr Robert Brooks
TRW Systems Group
R1/1062 One Space Park
Redondo Beach, California 90278

Dr. F. Paul Carlson, President
Oregon Graduate Center
19600 N. W. Walker Road
Beaverton, Oregon 97005

Prof W. Thomas Cathey
Dept of Electrical Engineering
University of Colorado
Denver, Colorado 80302

Dr H. J. Caulfield
Aerodyne Research, Inc
Applied Science Division
Bedford Research Park
Bedford, Massachusetts 01730

Dr Edwin Champagne
AFAL/DH
Wright-Patterson AFB, Ohio 45433

Prof Stuart A. Collins, Jr
Dept of Electrical Engineering
Ohio State University
2015 Neil Avenue
Columbus, Ohio 43210

Dr Nabil Farhat
University of Pennsylvania
200 South 33rd Street
Philadelphia, Pennsylvania 19174

Dr David Flannery
Mr Mike Hamilton
AFAL/DHO
Wright-Patterson AFB, Ohio 45433

Dr Albert Friesem
Weizmann Institute of Science
Rehovot, Israel

Dr. B. D. Guenther
Physics Division
U. S. Army Research Office
Post Office Box 12211
Research Triangle Park
North Carolina 27709

Dr Richard Hudgins
Itek Corporation
10 Maguire Road
Lexington, Massachusetts 02173

Dr T. C. Lee
Corporate Research Center
Honeywell, Inc.
10701 Lyndale Ave., So.
Bloomington, Minnesota 55420

Prof Adolf Lohmann
Physics Institute
University of Erlangen-Nurnberg
Erwin-Rommel-Strasse
D 8520 Erlangen
F.R. Germany

Mr Bob V. Markevitch
Ampex Corporation
401 Broadway
Redwood City, California 94063

Dr Robert Marks
Dept of Electrical Engineering
University of Washington
Seattle, Washington 98195

Captain Bill Miceli
RADC/ESO
L. G. Hanscom AFB, Massachusetts 01730

Dr Robert A. Sprague
Xerox Corporation
Palo Alto Research Labs
3333 Coyote Hill Road
Palo Alto, California 94304

Mr Eric Stevens
Code 7924S
Naval Research Laboratory
Washington, D.C. 20375

Dr William Stoner
Systems Applications, Inc.
3 Preston Court
Bedford, Massachusetts 01730

Dr. Henry Taylor
Naval Research Lab.
Washington, D. C.

Prof Brian Thompson, Dean
School of Engineering
University of Rochester
Rochester, New York 14627

Mr Terry Turpin
NSA R551
9800 Savage Road
Fort Meade, Maryland 20755

Dr Anthony Vander Lugt
232 Cocoa Avenue
Indialantic, Florida 32903

Dr Bernard Vatz, Radar Directorate
BMDATC
P. O. Box 1500
Huntsville, Alabama 35807

Dr Carl M. Verber
Battelle Columbus Laboratories
505 King Avenue
Columbus, Ohio 43201

Mr Harper Whitehouse
Naval Ocean Systems Center
San Diego, California 92152

Prof James Wyant
Optical Sciences Center
University of Arizona
Tucson, Arizona 85721

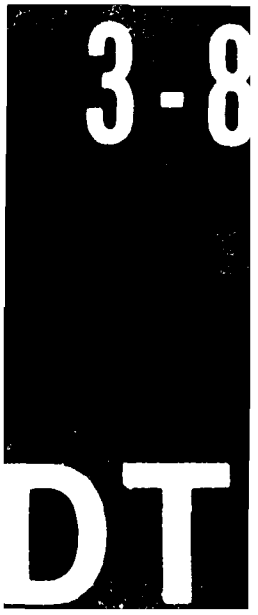
3-8
DT